ORIGINS OF MASS-DEPENDENT AND MASS-INDEPENDENT Ca ISOTOPE VARIATIONS IN METEORITIC COMPONENTS. K.R. Bermingham[1,2], N. Gussone[2], and K. Mezger[2,3], [1]Isotope Geochemistry Laboratory, Department of Geology, University of Maryland, College Park, MD-20740 USA (kberming@umd.edu), [2]Institut für Mineralogie, Westfälische Wilhelms-Universität, Corrensstraße 24, Münster, 48149 Germany, [3]Institut für Geologie, Universität Bern, Baltzerstrasse 1 + 3, Bern, 3012 Switzerland.

Introduction: Mass-dependent Ca isotope effects ($\delta^{44/40}$Ca) in calcium aluminum inclusions (CAIs) likely developed via kinetic isotope-fractionation during condensation, which was induced by a complex series of thermal processing events [1-6]. This is supported by the correlation between highly fractionated Group II rare earth element (REE) abundance patterns and light $\delta^{44/40}$Ca compositions [4], where "light" refers to $\delta^{44/40}$Ca values that are less than $\delta^{44/40}Ca_{BSE}$ +1.05 ±0.04 (BSE = bulk silicate Earth; [7]).

Here, the $\delta^{44/40}$Ca compositions of 16 different CAIs, chondrules, amoeboid olivine aggregates (AOAs), and dark inclusions from Allende (CV3) and NWA 753 (R3.9) are reported. Rare earth element abundance data on most samples were also collected. This is the first dataset to include $\delta^{44/40}$Ca data from AOAs and dark inclusions; and, the new chondrule data add nearly ~40 % to the published $\delta^{44/40}$Ca chondrule database [6,8]. The origin of these $\delta^{44/40}$Ca compositions are investigated, including the potential relationship between volatility controlled fractionation of REEs and $\delta^{44/40}$Ca compositions in AOAs and chondrules.

In addition to mass-dependent Ca isotope anomalies, mass-independent (or nucleosynthetic) $^{40/44}$Ca, $^{43/44}$Ca, $^{46/44}$Ca, and $^{48/44}$Ca isotope anomalies have been identified in presolar grains, meteoritic components, and whole rock meteorites [e.g., 1, 4, 9, 10]. Nucleosynthetic Ca isotope heterogeneity likely reflects the incomplete homogenization of nucleosynthetic materials [4, 11], or, the selective unmixing of at least two presolar grain dust generations with contrasting thermal and/or physical properties [12]. Here, the origin of $^{48/44}$Ca signatures in CAIs, chondrules, AOAs, and dark inclusions is probed by exploring the relationship between their $\delta^{44/40}$Ca *vs.* $\varepsilon^{48/44}$Ca compositions.

Samples: Five AOAs (AOA 1-5), five chondrules (C 1-4,6), and a CAI (CAI 5) were isolated using a dental burr from a ~5.5 g sample of Allende provided by the Natural History Museum (London, UK). Two CAIs (CAI 1 and CAI 2) and one dark inclusion (DI 1) were isolated from a piece of Allende provided by the Institut für Planetologie, Westfälische Wilhelms-Universität (WWU) (Münster, DE). Two dark inclusions (DI 2 and DI 3) were isolated from a piece of NWA 753 (R3.9) provided by WWU.

Methods: Detailed methods are provided in [13]. Briefly, after complete digestion and when sample mass permitted, samples were split into two separate fractions for the measurement of mass-dependent and mass-independent Ca isotope effects. A ^{42}Ca-^{43}Ca double spike was applied for determination of mass-dependent effects, following [12-14]. Calcium isotope purification was completed following [15].

Calcium isotope measurements were performed using the *Thermo Fisher Triton* thermal ionization mass spectrometer at WWU. For spiked measurements, Ca isotope data are reported as $\delta^{44/40}$Ca (relative to SRM915a). Sample data were normalized to the average SRM915a composition of the respective analytical campaign, where replicate analyses of the SRM915a standard define a 2SD external precision $\delta^{44/40}$Ca ±0.15 to ±0.18 ‰. For unspiked measurements, Ca isotope ratios were corrected for mass-dependent fractionation using the Rayleigh law, the masses of monoatomic Ca isotope species, and reference ratio ^{42}Ca/^{44}Ca = 0.31221 [16]). Data are reported in epsilon units (ε, relative to SRM915a). Replicate analyses of SRM915a standard define a 2SD external precision of $\varepsilon^{40/44}$Ca ±3.66, $\varepsilon^{43/44}$Ca ±2.10, and $\varepsilon^{48/44}$Ca ±3.80.

Where sample size permitted, relative REE abundances were obtained using a *Thermo Finnigan* ELEMENT 2 single collector inductively coupled plasma mass spectrometer in solution mode at the University of Maryland, College Park (US).

Results: Most $\delta^{44/40}$Ca compositions are analytically resolved from $\delta^{44/40}Ca_{BSE}$, varying within and between sample types [13]. The CAI and chondrule $\delta^{44/40}$Ca compositions concur with published data [4,6,8]. CAIs have light $\delta^{44/40}$Ca compositions whereas chondrules are either heavy or light. The average chondrule composition is analytically identical to BSE, in agreement with [6,8]. Amoeboid olivine aggregates have light $\delta^{44/40}$Ca compositions and are less variable in composition than CAIs. Dark inclusions are generally heavier than BSE and have restricted $\delta^{44/40}$Ca compositions. All samples have normal $\varepsilon^{40/44}$Ca, $\varepsilon^{43/44}$Ca, and $\varepsilon^{48/44}$Ca compositions, except AOA 1, AOA 5, C 2, and C 4 which have anomalous $\varepsilon^{48/44}$Ca compositions (Fig. 1).

The CI normalized REE pattern for C 2 shows depletions in Ce, Eu, and Yb and is classified as Group I-An. The CI normalized REE pattern of CAI 5 shows an enrichment in LREE relative to HREE, except for Tm and Yb which are approximately equal in abundance to the LREE. This pattern is similar to Modified Group II patterns [4] and CAI 5 is classified here as Group II-A. The remaining samples have flat CI normalized REE patterns.

Discussion: The Group II-A REE pattern and $\delta^{44/40}$Ca composition of CAI 5 suggests that this inclusion (or its precursor material) formed via condensation from a gas reservoir after up to 3 % of an ultrarefractory condensate had previously been removed from an originally chondritic reservoir (following [4]). The $\delta^{44/40}$Ca of C 2 is not very fractionated, suggesting that the thermal events causing depletion in Cs, Eu, and Yb did not reach high enough temperatures to extensively fractionate Ca isotopes. Huang et al. (2012) proposed that CAIs with flat REE patterns and chondritic $\delta^{44/40}$Ca compositions formed via the accretion of both the condensate and the ultrarefractory residue. This scenario may be extended to include chondrules. The moderate $\delta^{44/40}$Ca variation in chondrules and those CAIs with flat REE patterns may be the result of slightly imperfect mixing between phases that have highly variable $\delta^{44/40}$Ca compositions by virtue of their condensation from the compositionally different evaporative residue and condensate phases. Alternatively, the REE and $\delta^{44/40}$Ca compositions may have been decoupled from each other due to non-equilibrium condensation [3,6].

Unlike CAIs and chondrules, AOAs are aggregates of different mineral assemblages that formed under different nebular conditions [17]. The light $\delta^{44/40}$Ca composition and Group II-A REE fractionation pattern of AOA 1 may indicate that this component (or its precursor material) were established by the same thermal event, similar to CAI 5. This conclusion is tenuous, however, because the percentage of the Ca isotope composition and REE abundances originating from the refractory mineral assemblage is unknown.

The minor fractionation in $\delta^{44/40}$Ca in dark inclusions lends further support to the hypothesis that dark inclusions are variably altered fragments of CV3 chondritic materials that formed on the CV parent body and not aggregates of nebular condensates [18].

Schiller et al., (2015) proposed that mass-independent Ca isotope anomalies in meteorites are a consequence of the selective unmixing of two homogeneously distributed components via sublimation of thermally unstable isotopically anomalous presolar carriers. If so, this effect may be apparent in a correlation between mass-independent and mass-dependent Ca isotope compositions, where heavy $\delta^{44/40}$Ca signatures would be coupled with $\varepsilon^{48/44}$Ca anomalies. Data from the present study and [4] are shown in Fig. 1. It is difficult to assess the presence of a correlation given the current limited dataset, however, it can be concluded that a strong correlation is not apparent. This is in contrast to recently reported Ti isotope data [19] where it was noted that samples with the largest mass-independent Ti isotope anomalies tend to have the most dispersion in mass-dependent Ti isotope compositions. The absence of a strong correlation between $\delta^{44/40}$Ca *vs.* $\varepsilon^{48/44}$Ca in the current dataset suggests that the thermal processing event that caused $\varepsilon^{48/44}$Ca anomalies likely did not concurrently establish the $\delta^{44/40}$Ca compositions in these meteorite components.

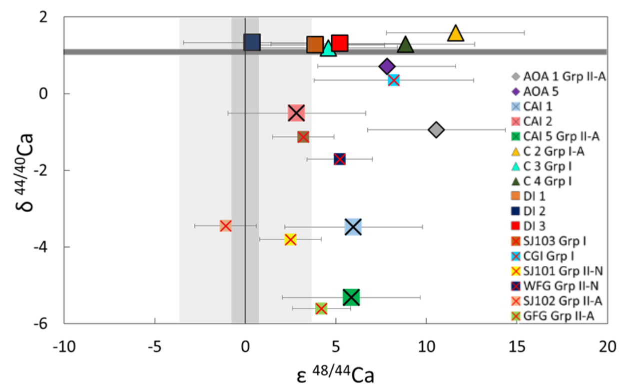

Fig. 1. $\delta^{44/40}$Ca *vs.* $\varepsilon^{48/44}$Ca for CAIs, AOAs, chondrules, and dark inclusions from present study and [4]. Estimate for $\delta^{44/40}Ca_{BSE}$ ~1.05±0.04 [7] is shown as the darkest grey horizontal bar. Vertical grey fields represent the $\varepsilon^{48/44}$Ca external precision reached in the present study (light grey) and [4] (dark grey).

References: [1] Niederer F.R. and Papanastassiou D.A. (1984) *GCA*, *48*, 1279-1293. [2] MacPherson et al. (1988) *Meteorites and the Early Solar System*, 746-807. [3] Simon J.I. and DePaolo D.J. (2010) *EPSL*, *289*, 457-466. [4] Huang S. et al. (2012) *GCA*, *77*, 252-265. [5] Zhang J. et al. (2014) *GCA*, *140*, 365-380. [6] Simon J.I. et al. (2017) *EPSL*, *472*, 277-288. [7] Huang S. et al. (2010) *EPSL*, *282*, 337-344. [8] Amsellem E. et al., (2017) *EPSL*, *469*, 75-83. [9] Lee T. et al. (1978) *Ap. J.*, *220*, L21-L25. [10] Papanastassiou D.A. and Brigham C. (1989) *Ap. J.*, *338*, L37-40. [11] Dauphas N. et al. (2014) *EPSL*, *407*, 96-108. [12] Schiller M. et al. (2015) *GCA*, *149*, 88-102. [13] Bermingham K.R. et al. (in revision in *GCA*). [12] Gussone N. et al. (2011) *Chem. Geol.*, *285*, 194-202. [13] John T. et al. (2012) *Nature Geosci.*, *5*, 489-492. [14] Magna T. et al. (2015) *EPSL*, *430*, 86-94. [15] Ockert C. et al. (2013) *GCA*, *112*, 374-388. [16] Russell W.A. et al. (1978) *GCA*, *42*, 1075-1090. [17] Ruzicka A. et al. (2012) *GCA*, *79*, 79-105. [18] Krot A.N. et al. (2000) *Geochem. Intl.*, *38*, S351-S368. [19] Davis A.M. et al. (2017) *GCA*, *221*, 275-295.